Distribution of Metals and Toxic Elements Between Carbonate, Sulfate, and Oxide Mineral Precipitates

Julie J. Kim[1], Satish C.B. Myneni[2], Catherine A. Peters[1]

[1]Department of Civil & Environmental Engineering, Princeton University, Princeton, NJ, 08544, juliejk@princeton.edu

[2]Department of Geosciences, Princeton University, Princeton, NJ, 08544

Abstract

Immobilization of toxic elements from pH adjusted sulfidic mine waters via coprecipitation in carbonate minerals was studied. To design toxic metal mitigation efforts and to assess permanence, it is important to know how trace elements distribute between mineral precipitates of different reactivity and stability under environmental conditions. Experiments using synthetic mine waters were conducted and various imaging and analytical approaches were coupled to image and quantify trace element uptake in precipitated mineral phases. In the copresence of carbonate and oxide minerals, or carbonate and sulfate minerals, cadmium and zinc concentrations were consistently higher in calcium carbonate phases and demonstrated patterns of coprecipitation.

Keywords: Toxic Metals, Mine Waste, Mine Drainage, Mineral Coprecipitation, Solid Solution

Introduction

Sulfide-based mines are ubiquitous in the U.S. and worldwide, yet beneficial reuse or carbonation of these mine wastes is limited. Motivated by the successful pilot and full-scale carbon mineralization projects in ultramafic or alkaline mines (Kelemen *et al.* 2020), we consider carbonation scenarios in sulfidic mines. The evident drawback of the low pH conditions can be overcome by considering low-cost or recycled alkaline additives. To date, many different alkaline materials, and wastes such as fly ash, red mud, steel slag, have been chemically and mineralogically characterized and quantified in terms of their carbonation potential (Renforth 2019; Catalano *et al.* 2012). With carbonate precipitation, toxic metals and metalloids (e.g., lead, cadmium, arsenic, zinc, etc.) may also be coprecipitated out in the form of solid solutions, for the dual benefit of carbon mineralization and toxic metal mitigation. Relevant observations were reported in the case of carbonation of fly ash leachates, which led to trace metal-bearing calcium carbonate precipitates (Hunter *et al.* 2021). With the formation of metal-bearing carbonates, achieving permanency of the treatment is critical and any risks associated with carbonate redissolution, such as new acidity generation from the oxidation and dissolution of sulfides, must be minimized. New acidity generation is expected to be offset by co-disposed or blended alkaline additives, yet this needs to be carefully engineered.

Recent literature has shown that by coprecipitation, metals and metalloids can be precipitated out even at concentrations below saturation of the respective end members, by scavenging their way into the dominant end-member phase. Prieto *et al.* (2016) demonstrated that in the case of solid solution $((Ca,Cd)CO_3)$ precipitation, cadmium concentrations remaining in solution were nearly 2 orders of magnitude lower than in the case of only otavite $(CdCO_3)$ precipitation. Hunter *et al.* (2021) also found that thermodynamic models of solid solution precipitation significantly underestimated the extent of trace metal incorporation. For As, Cr, Zn, and Cu, it was found that the ratio of observed concentrations (in the solid) to thermodynamically predicted concentrations (in the solid) ranged anywhere between 5 and 3000 (Hunter *et al.*, 2021). With this, it is likely that coprecipitation reactions serve a much bigger role in toxic component uptake from solution than previously predicted.

In this work, we tested various carbonation scenarios in batch experiments involving synthetic mine waters to test if toxic metal concentrations can be minimized and fall below acceptable water concentrations (as set by the U.S. EPA). The metals and metalloids we selected as trace elements were Pb, Zn, As and Cd, and we designed the experiment to involve oxidized forms of sulfur (VI) and iron (III), and calcium and carbon to enable simultaneous precipitation of sulfate, iron oxide and/or carbonate minerals. To comment on the stability and permanency of the element uptake, we mapped out how the four elements distributed between carbonate, sulfate, or (oxy)hydroxide phases, since these are minerals that exhibit different degrees of reactivity and stability. We also showed which phase(s) are most effective at element uptake and whether they formed binary or ternary solid solutions.

Methods

A series of batch experiments were set up at room temperature using salts of the desired cations and anions. Oxidized forms of As (V), Fe (III) and SO_4 salts were added, and reactions were carried out in vials open to the atmosphere. Geochemical modeling software, PHREEQC (Parkhurst and Appelo 2013), was used to determine the ratio of major cations (calcium and iron) and anions (carbonate, sulfate) as well as the pH that would lead to specific mineral phases or a set of phases to study the extent of uptake as well as the distribution of elements among the phases formed. The phases of interest are three polymorphs of Ca-carbonates (calcite, vaterite, or aragonite which are the expected products of carbonation, Fe- and Ca-sulfate phases (natrojarosite and gypsum), which are two of the most common oxidized sulfur-bearing phases in mining environments, and iron-oxyhydroxide phases. Mine water composition data from gold, copper, coal, silver, uranium, or sulfur mines were compiled from the literature, and initial concentrations of the minor elements in our experiments (As, Cd, Pb, and Zn) were selected to fall within reported ranges. The initial concentrations of the trace elements are summarized in Table 1. These concentrations (with the exception of zinc) exceed the U.S.EPA's maximum allowable concentrations according to drinking water regulations of the Safe Drinking Water Act. Treated solutions were collected after 1-week, and solution samples were acidified with nitric acid for Inductively Coupled Plasma - Mass Spectrometry (ICP-MS) analysis. Solid precipitates were three times DI-washed and twice ethanol-washed and dried for

Table 1 Summary of initial conditions and final solution ICP-MS data for select batches.

| Case		pH_{init}	Initial (mol/L)	Final (mol/L)	% decrease	U.S.EPA standards (mol/L)
Carbonate & Sulfate (C1)	As	7	0.002	6.83E-05	> 95	0.0001
	Cd		0.001	5.19E-06	> 99	0.00007
	Zn		0.002	1.96E-06	> 99	0.08
	Pb		0.001	6.70E-08	> 99	0.00004
Carbonate & Oxide (C2)	As	7		5.07E-07	> 99	
	Cd			3.07E-06	> 99	
	Zn			1.99E-06	> 99	
	Pb			9.35E-08	> 99	
Sulfate only (C3)	As	4		3.95E-04	> 74	
	Cd			7.15E-04	> 32	
	Zn			1.01E-03	> 38	
	Pb			5.00E-04	> 5	
Sulfate & Oxide (C4)	As	4		6.66E-07	> 99	
	Cd			9.23E-04	> 14	
	Zn			1.10E-03	> 33	
	Pb			2.65E-04	> 53	

X-ray Diffraction (XRD) and Scanning or Transmission Electron Microscopy (S(T)EM) analyses.

Results and Discussion

After a 1-week period, all metal and metalloid concentrations in the two carbonated batches (C1 and C2), were decreased by >99% for all cases, except As in case C1, which decreased by approximately 95% (Table 1). Carbonation led to carbonate precipitates that effectively reduced metal(loid) concentrations from the solution, leading to treated solutions that fell well below the maximum limit set by the U.S.EPA. Non-carbonated, or sulfate and oxide precipitated batches (C3 and C4) showed variable decreases in concentrations. The data most prominently captures reduced effectiveness of Pb, Cd, and Zn uptake from the solution without carbonate precipitation. In terms of the solid phases, XRD analyses showed presence of vaterite (C1), calcite (C2), gypsum (C1 and C4), Fe (III)-oxide (C2 and C4), and Natrojarosite (C3).

In case C1 of simultaneous calcium carbonate and gypsum precipitation, vaterite was the dominant polymorph of calcium carbonate that was observed. Spherical vaterites were found in the solution and many were found attached to the needle structures of the gypsum as seen in Figure 1a. It is unknown whether the vaterite precipitated on the gypsum needles (using it as a substrate) or formed in solution and later attached to the gypsum. The TEM image (Figure 1b) and element distribution maps of As, Zn, and Cd (Figure 1c-e) highlight the distinct spherical morphology of vaterite and the spatial distribution of three elements in the crystal. Lead is not mapped because it was detected at very low concentrations. Zinc and cadmium maps show homogeneous distribution of the elements throughout the spherical particle, indicating coprecipitation as the mechanism of uptake in the solid. Other possible mechanisms of uptake include adsorption of ions on the surface, or precipitation of a new, secondary phase on the surface. Arsenic shows both a spotty and a homogeneous distribution within the particle, and this trend suggests simultaneous distribution of arsenic in the crystal and on the surface, coming from either precipitation of new phases or adsorption. Figure 1f of quantitative solid phase EDS data highlights the apparent metal(loid) distribution between vaterite and gypsum. The affinity of As, Cd, and Zn to associate with vaterite over gypsum is clearly observed, while for Pb, this trend is not so clear. Pb incorporation into vaterite may be less favorable because Pb forms an aragonite group end member phase, cerussite ($PbCO_3$), and this phase is also the least soluble phase of the three carbonate endmembers (Zn, Cd, and Pb-carbonates).
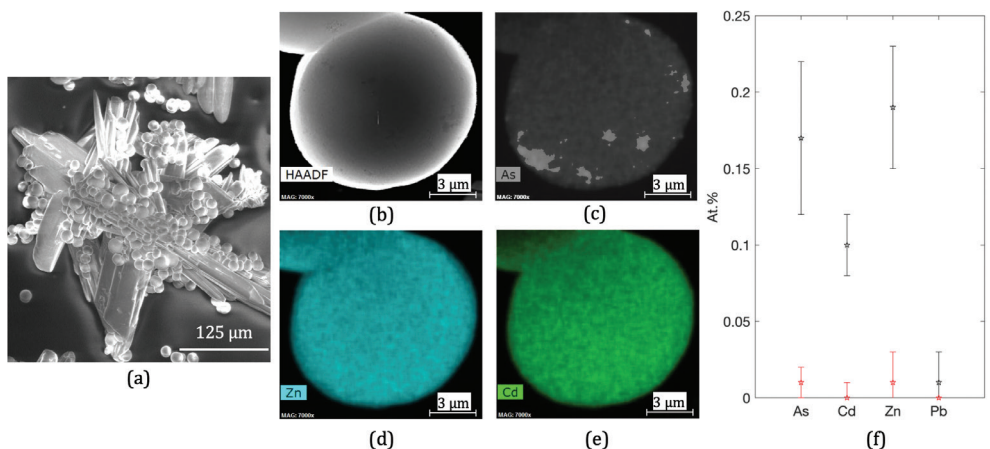
Figure 1 (a) SEM image of precipitated gypsum and spherical vaterite crystals from C1. (b) STEM image, and single particle EDS element map of (c) arsenic, (d) zinc, and (e) cadmium. Lead map is not shown because it was detected at very low concentrations. (f) Plot of atomic % vs. elements, highlighting the extent of metal incorporation in calcium carbonate (black) and gypsum (red).

SEM-EDS analysis of the solids formed in case C2 of simultaneous carbonate and oxide precipitation shows a clear division of elements between the two phases (Table 2). The calcite phase shows higher concentrations of Cd and Zn, while the Fe (III) phase shows higher concentrations of As and Pb. While EDS mapping of iron and oxygen (Figure 2) show numerous hotspots of the two elements supporting the probable formation of iron (oxy)hydroxide, we could not identify the specific crystalline Fe (III) phase from our XRD analyses. This may due to the formation of amorphous iron phases or thin iron-(oxy) hydroxide coatings that did not produce identifiable peaks in our XRD patterns.

In the calcite phase, we analyzed both the outer surface and a fractured surface for the elemental presence, and we found significantly higher atomic % of Zn and Cd on the fractured surface than the outer surface. This serves as good evidence for coprecipitated Cd and Zn in the calcite phase. The similarity in the crystal group of otavite ($CdCO_3$), Smithsonite ($ZnCO_3$), and calcite is one likely explanation for the strong affinity of Cd and Zn to associate with calcite. Cerussite forms an aragonite group crystal structure (orthorhombic), and arsenate forms a calcium arsenate phase, where the crystal structure differs significantly from the calcite group, thus reducing ease or likelihood of coprecipitation. For the iron (III) phase, we can predict that there may be some competition between coprecipitation and adsorption, as iron oxides are well known for their effective adsorption capacities. Residual As and Pb concentrations in the solution may be adsorbing to the oxide phase after

Table 2 Summary of element incorporation in Fe (III) phase and calcite from C2.

Element	Fe (III) Phase: At. % ± Stdev	Calcite: At. % ± Stdev
As	0.33±0.05	0.02±0.04
Cd	0.11±0.02	0.32±0.09
Zn	0.22±0.07	0.44±0.11
Pb	0.13±0.03	0.02±0.03

precipitation. Another notable feature from this batch is the codetection of Ca and C in the Fe (III) phase spots (see EDS data box in Figure 2a). This could be indicative of calcite crystals coated with an iron oxide layer, an observation that is quite desirable for these carbonation scenarios, as iron oxides could serve as a protective layer for the calcium carbonates.

Two different sulfate phases were observed in cases C3 and C4, and these phases were identified by XRD as natrojarosite and gypsum, respectively (Figure 3). Solid phase analyses showed strong arsenic association with the natrojarosite phase in case C3, and this is also supported by the largest percentage decrease in arsenic concentration in the solution after 1 week (Table 1). Arsenic associations with jarosite group minerals have also been observed and reported in the literature. Hudson-Edwards (2019) found that arsenate oxyanions can substitute for sulfate groups in the T-site of the jarosite structure, leading to arsenojarosite phases of varying arsenate to sulfate ratios.

For the gypsum observed in case C4, formation of an iron oxide coating is clear from SEM-EDS analyses of some select spots (Figure
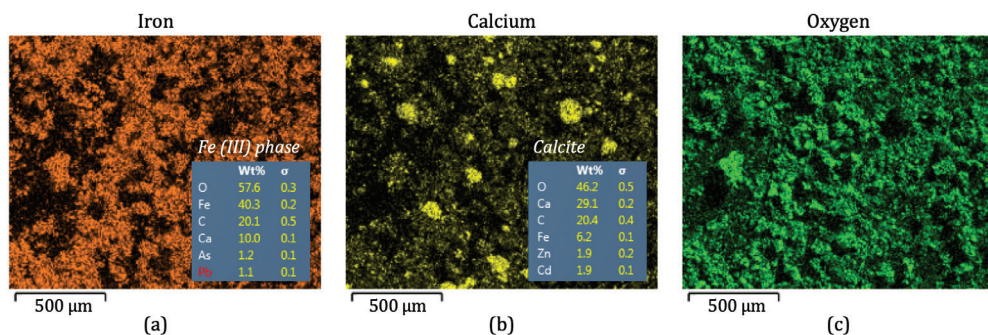
Figure 2 EDS element maps of (a) iron, (b) calcium, and (c) oxygen from C2 solids. Blue boxes summarize the elemental composition from one point in the map.

3b and 3c), and there is some preliminary evidence that minor element (Pb and As) concentrations are locally higher in these Fe rich regions. (Figure 3c). This observation of Fe (III) phase and Pb and As association agrees well with results presented for case C2 and is also supported by the solution data for C4 presented in Table 1.

From the proposed in-situ carbonation in mine waste sites, it is expected that there will be large volumes of precipitates generated, further motivating us to consider reutilization of the precipitated carbonates. However, the products created will be classified as high-volume, low-end, as defined by Sanna *et al.* (2015), due to the incorporated toxic components. This could limit direct application of the precipitates in the field (e.g., use as liming agents or soil additives) because there is risk of re-release of the toxic components into the environment. However, if analysis of the metal(loid) concentration shows to be low enough, mixing with other pure liming agents for diluted application in soils or other acidic settings may be appropriate. Alternatively, we can consider applications in concrete production or use as paint additives. The different morphologies and polymorphs of calcium carbonates observed in these systems can be taken advantage of in terms of serving different functions in paint such as dispersion, brightness, transparency, etc. (Li *et al.* 2013).

Conclusions

Carbonation in sulfidic mine waters will induce new sets of reactions, including carbonate coprecipitation reactions, and we showed through our experimental results that toxic components in synthetic mine waters were effectively minimized under these carbonation scenarios via the formation of metal and metalloid bearing carbonates. Carbonates were the most effective phase in uptake of Cd and Zn, and we observed formation of ternary solid solutions. In the copresence of oxide and calcium carbonate, we observed Cd and Zn in the carbonate phase, and As and Pb in the oxide phase. Efficacy of carbonation for simultaneous CO_2 mineralization and metal uptake in Zn or Cd mines is expected to be high, while other treatment methods may be favorable for mines rich in Pb or As. Additional analyses on the overall stability of the system or the reactivities of the coprecipitated crystals remain to be analyzed in greater depths in future works. Finding the conditions that would minimize, if not mitigate, the potential for redissolution of the precipitated carbonates is a major consideration in the context of sulfidic mines, and achievement of shielded carbonate precipitation may be a solution for this.
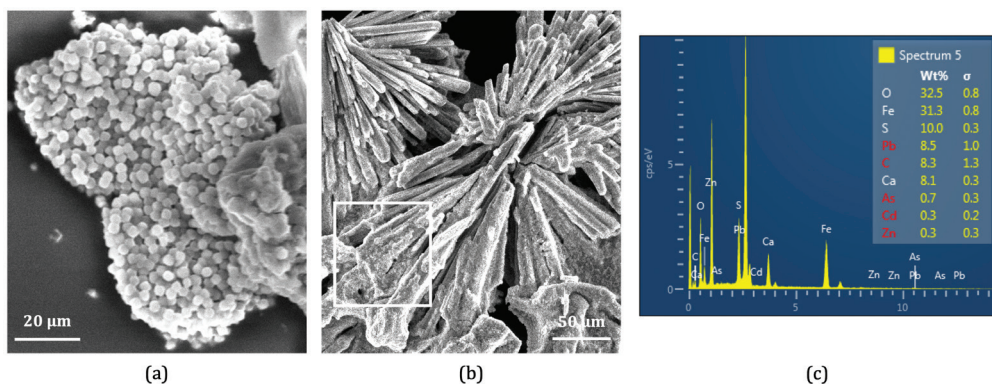
Acknowledgements

Figure 3 *SEM image of (a) precipitated Na-jarosite from C3 and (b) Fe-coated gypsum from C4, with the iron-rich region marked by the white box. (c) Point EDS spectra from the white boxed region.*

References

Hunter HA, Ling FT, Peters CA (2021) Coprecipitation of Heavy Metals in Calcium Carbonate from Coal Fly Ash Leachate. ACS ES&T Water 1:339–345. https://doi.org/10.1021/acsestwater.0c00109

Prieto M, Heberling F, Rodríguez-Galán RM, Brandt F (2016) Crystallization behavior of solid solutions from aqueous solutions: An environmental perspective. Prog Cryst Growth Charact Mater 62:29–68. https://doi.org/10.1016/j.pcrysgrow.2016.05.001

Kelemen PB, McQueen N, Wilcox J, *et al* (2020) Engineered carbon mineralization in ultramafic rocks for CO2 removal from air: Review and new insights. Chem Geol 550:119628. https://doi.org/10.1016/j.chemgeo.2020.119628

Catalano JG, Huhmann BL, Luo Y, *et al* (2012) Metal release and speciation changes during wet aging of coal fly ashes. Environ Sci Technol 46:11804–11812. https://doi.org/10.1021/es302807b

Renforth P (2019) The negative emission potential of alkaline materials. Nat Commun 10:1401. https://doi.org/10.1038/s41467-019-09475-5

Sanna A, Uibu M, Caramanna G, Kuusik R, Maroto-Valer M.M (2014) A review of mineral carbonation technologies to sequester CO2. Chem Soc Rev 43:8049–8080. https://doi.org/10.1039/c4cs00035h

Li G, Li Z, Ma H (2013) Synthesis of aragonite by carbonization from dolomite without any additives. Int J Miner Process 123:25–31. https://doi.org/10.1016/j.minpro.2013.03.006

Hudson-Edwards, KA (2019). Uptake and release of arsenic and antimony in alunite-jarosite and beudantite group minerals. American Mineralogist, 104(5), 633–640. https://doi.org/10.2138/am-2019-6591

Parkhurst DL, Appelo CA (2013). Description of input and examples for PHREEQC version 3–A computer program for speciation, batch-reaction, one-dimensional transport, and inverse geochemical calculations, volume book 6 series Techniques and Methods. https://pubs.usgs.gov/tm/06/a43.